
Synthesis of ^{18}F -Tetrafluoroborate via Radiofluorination of Boron Trifluoride and Evaluation in a Murine C6-Glioma Tumor Model

Huailei Jiang¹, Aditya Bansal¹, Mukesh K. Pandey¹, Kah-Whye Peng², Lukkana Suksanpaisan³, Stephen J. Russell², and Timothy R. DeGrado¹

¹Department of Radiology, Mayo Clinic, Rochester, Minnesota; ²Department of Molecular Medicine, Mayo Clinic, Rochester, Minnesota; and ³Imanis Life Sciences, Rochester, Minnesota

The sodium/iodide symporter (NIS) is under investigation as a reporter for noninvasive imaging of gene expression. Although ^{18}F -tetrafluoroborate (^{18}F -TFB, ^{18}F - BF_4^-) has shown promise as a PET imaging probe for NIS, the current synthesis method using isotopic exchange gives suboptimal radiochemical yield and specific activity. The aim of this study was to synthesize ^{18}F -TFB via direct radiofluorination on boron trifluoride (BF_3) to enhance both labeling yield and specific activity and evaluation of specific activity influence on tumor uptake. **Methods:** An automated synthesis of ^{18}F -TFB was developed whereby cyclotron-produced ^{18}F -fluoride was trapped on a quaternary methyl ammonium anion exchange cartridge, then allowed to react with BF_3 freshly preformulated in petroleum ether/tetrahydrofuran (50:1). The resultant ^{18}F -TFB product was retained on the quaternary methyl ammonium anion exchange cartridge. After the cartridge was rinsed with tetrahydrofuran and water, ^{18}F -TFB was eluted from the cartridge with isotonic saline, passing through 3 neutral alumina cartridges and a sterilizing filter. Preclinical imaging studies with ^{18}F -TFB were performed in athymic mice bearing NIS-expressing C6-glioma subcutaneous xenografted tumors to determine the influence of specific activity on tumor uptake. **Results:** Under optimized conditions, ^{18}F -TFB was synthesized in a radiochemical yield of $20.0\% \pm 0.7\%$ ($n = 3$, uncorrected for decay) and greater than 98% radiochemical purity in a synthesis time of 10 min. Specific activities of 8.84 ± 0.56 GBq/ μmol ($n = 3$) were achieved from starting ^{18}F -fluoride radioactivities of 40–44 GBq. An avid uptake of ^{18}F -TFB was observed in human NIS (hNIS)-expressing C6-glioma xenografts as well as expected NIS-mediated uptake in the thyroid and stomach. There was a positive correlation between the uptake of ^{18}F -TFB in hNIS-expressing tumor and specific activity. **Conclusion:** A rapid, practical, and high-specific-activity synthesis of the NIS reporter probe ^{18}F -TFB was achieved via direct radiofluorination on BF_3 using an automated synthesis system. The synthesis of high-specific-activity ^{18}F -TFB should enable future clinical studies with hNIS gene reporter viral constructs.

Key Words: sodium/iodide symporter; tetrafluoroborate; ^{18}F ; PET; radiofluorination

J Nucl Med 2016; 57:1454–1459
DOI: 10.2967/jnumed.115.170894

The sodium/iodide symporter (NIS) is an intrinsic membrane glycoprotein, which mediates the uptake of iodide in the thyroid gland and other NIS-expressing cells or tissues (1–3). The active transport of iodide is the basis for the diagnosis and therapeutic treatment of thyroid disease and thyroid cancer. The clinical application of radioiodine also builds the foundation of modern nuclear medicine (4). The identification and characterization of human NIS (hNIS) in 1996 (5,6) created new opportunities for the use of hNIS as a reporter gene in viral therapy investigations and imaging of cell migration and differentiation. Despite considerable success in single-photon imaging of thyroid and thyroid cancers with ^{123}I , ^{131}I , or $^{99\text{m}}\text{Tc}$ -pertechnetate (2,3), there remain obvious limitations for use of these radioisotopes for diagnostic imaging. Both ^{123}I (half-life [$T_{1/2}$] = 13.13 h) and ^{131}I ($T_{1/2}$ = 8.02 d) are true iodine imaging radiotracers but have longer half-lives than required for a diagnostic study, which result in an unnecessarily high dose of irradiation to patients and staff. $^{99\text{m}}\text{Tc}$ -pertechnetate ($T_{1/2}$ = 6 h) has found use as a radioiodine analog in thyroid diseases (7,8) and has suitable properties for SPECT. Nevertheless, SPECT has limited resolution and sensitivity, especially in detection of small metastases and low-volume diseases. PET has significantly better sensitivity and quantitative accuracy than SPECT, particularly for accumulations in small regions. The positron emitter ^{124}I ($T_{1/2}$ = 4.2 d) has been used in NIS imaging (9). However, the unnecessarily long half-life of ^{124}I and its complex emission properties that include high-energy γ -photons are drawbacks for diagnostic imaging applications. Also, the production of ^{124}I requires specialized solid target systems, which are not available in most cyclotron facilities (10). Positron-emitting ^{18}F -fluoride (^{18}F , $T_{1/2}$ = 109.7 min) is the most commonly used radioisotope for PET imaging. It has favorable physical decay properties of 97% positron emission and low positron energy ($\beta^+_{\text{max}} = 0.635$ MeV) and is produced by all PET cyclotrons. The development of ^{18}F -fluoride-based PET tracers for NIS imaging would be encouraging. Because various anions (e.g., I^- , SeCN^- , SCN^- , ReO_4^- , TcO_4^- , NO_3^-) are transported by NIS (6), the critical physicochemical

Received Dec. 11, 2015; revision accepted Mar. 14, 2016.
For correspondence or reprints contact either of the following:
Timothy R. DeGrado, Department of Radiology, Mayo Clinic, 200 First St. SW, Rochester, MN 55905.
E-mail: degrado.timothy@mayo.edu
Huailei Jiang, Department of Radiology, Mayo Clinic, 200 First St. SW, Rochester, MN 55905.
E-mail: Jiang.huailei@mayo.edu
Published online Apr. 21, 2016.
COPYRIGHT © 2016 by the Society of Nuclear Medicine and Molecular Imaging, Inc.

feature of these well-transported substrates is anionic monovalency with size and space-filling properties similar to the iodide ion. Before the advent of clinical PET, in the 1950s and early 1960s, Anbar et al. (11,12) reported that the tetrafluoroborate (TFB, BF_4^-) anion was effective to inhibit thyroid uptake of iodide ion. These researchers also showed that ^{18}F -labeled TFB, synthesized from reactor-produced ^{18}F -fluoride, specifically accumulated in rat thyroid. The initial labeling of TFB was accomplished by an ion exchange reaction of KBF_4 in acid at room temperature or heating to make ^{18}F -TFB, and the potassium salt was purified by recrystallization after neutralization (13). The isotopic exchange labeling approach inherently results in low-specific-activity ^{18}F -TFB. Recently, Jauregui-Osoro et al. (14) updated the labeling of ^{18}F -TFB using current ^{18}F -fluoride production and purification methods. With the same mechanism, ^{18}F -TFB was synthesized in a mixture of 1 mg of NaBF_4 and 1.5N hydrochloric acid at 120°C. ^{18}F -TFB of greater than 96% radiochemical purity was obtained in approximately 10% yield. The specific activity was approximately 1 GBq/ μmol , with starting activities of 12–18 GBq of ^{18}F -fluoride (14). PET/CT imaging in normal mice with transgenic thyroid tumors showed ^{18}F -TFB to delineate uptake in normal tissues expressing NIS (thyroid, stomach, salivary glands) and enhanced uptake in thyroid tumor. Researchers from the same institution also showed that ^{18}F -TFB was effective as a NIS probe in the NIS-transfected colon carcinoma cell line HCT116 (15). However, as pointed out by Youn et al. (16), specific activities achieved by the reported method are substantially lower than those typically required for receptor-mediated radiopharmaceuticals (~ 30 GBq/ μmol). In addition to this, a higher specific activity of ^{18}F -TFB (> 1 GBq/ μmol) is desired to avoid pharmacologic effects of administered TFB on iodine uptake in the thyroid (14). Therefore, it is of interest to develop a synthesis of ^{18}F -TFB with a higher specific activity. To perform PET imaging of NIS ultimately for clinical studies, our laboratory devoted efforts to synthesize high-specific-activity ^{18}F -TFB via the reaction of boron trifluoride (BF_3) and ^{18}F -fluoride. We herein report a successful method that uses automation and a quaternary methyl ammonium (QMA) anion exchange cartridge as a solid phase support for this reaction.

MATERIALS AND METHODS

General

Lewatit MP-64 chloride form resin was procured from Sigma Aldrich and converted to carbonate form. Acetone, tetrahydrofuran, and BF_3 were purchased from Sigma Aldrich. Petroleum ether was procured from Fisher Scientific. Sep-Pak Accell Plus QMA Carbonate Plus Light (46 mg of sorbent per cartridge, 40 μm particle size) and Alumina-N SepPak Light cartridges were obtained from Waters Corp. A Mini-scan radio-thin-layer chromatography (radio-TLC) scanner from Bioscan, Inc., was used to monitor the radiochemical purity. Anion high-performance liquid chromatography (HPLC) (IC-2100 [Dionex]; AS19 analytic column, 4.7 \times 150 mm; eluent 35 mM potassium hydroxide; sample volume, 25 μL ; flow rate, 1 mL/min) was calibrated to measure ^{19}F -TFB and ^{18}F -TFB concentrations with conductivity and radioactivity detectors in series. The method was validated by separation of a series of anions (F^- , Cl^- , Br^- , I^- , NO_3^- , CO_3^{2-} , and BF_4^-), and OH^- was negated by the system. Residual organic solvents were analyzed by gas chromatography (helium carrier gas flow at 10 mL/min through a MXT-WAX column [Restek; 0.53-mm inner diameter; 30-m length]). The temperature program was 4 min at 35°C, followed by a temperature ramp of 4°C per min to a maximum of 150°C.

^{18}F -TFB Synthesis Method

An automated synthesis of ^{18}F -TFB was developed for the preparation of ^{18}F -TFB (Fig. 1). ^{18}F -fluoride (37.6–40.5 GBq) was made by irradiation of 2.5 mL of ^{18}O -water with 65 μA for 15 min in a PETTrace

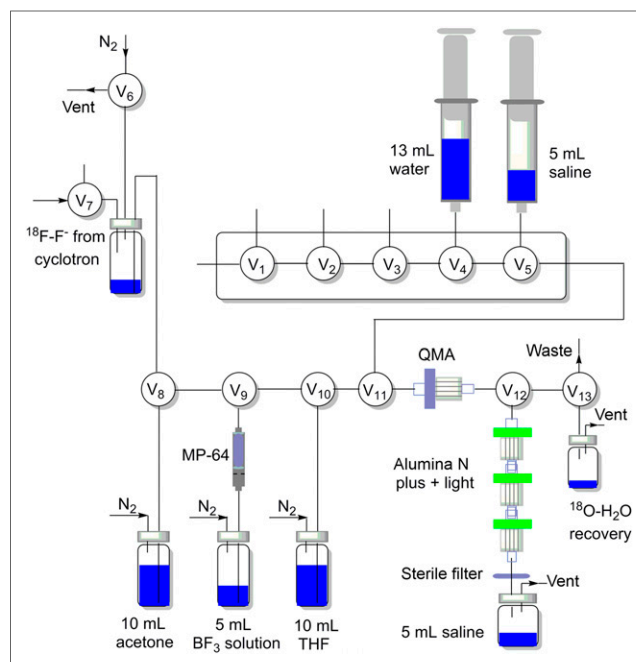


FIGURE 1. Schematic of automated module for preparation of ^{18}F -TFB. Valves V1–V5 are composed of single-use cassette that is mounted to front of module. All other valves are nondisposable Teflon diaphragm solenoid valves.

cyclotron (GE Healthcare) and then delivered to the hot cell and trapped on a QMA (46 mg, carbonate form) cartridge. ^{18}O -enriched water was collected using valve V13. The QMA cartridge was rinsed with 10 mL of anhydrous acetone and flushed with nitrogen for 100 s. The freshly prepared BF_3 –petroleum ether/tetrahydrofuran (50:1) solution (5 mL; supplemental data [supplemental materials are available at <http://jnm.snmjournals.org>]; Fig. 1) was filtered by an in-house-made Lewatit MP-64 cartridge (200–400 mg; supplemental data; Fig. 2) and then passed through the QMA cartridge within 10 s to react with the trapped ^{18}F -fluoride to form ^{18}F -TFB. The QMA cartridge was rinsed with a solution of 10 mL of tetrahydrofuran, flushed for 100 s with nitrogen, and rinsed with 13 mL of water to further remove impurities. The crude ^{18}F -TFB product was eluted from QMA with 5 mL of sterile 0.9% NaCl, U.S. Pharmacopeia solution (saline), and was further purified from unreacted ^{18}F -fluoride by passing through 3 alumina-N SepPak Light cartridges. After passage through a 0.2- μm sterilizing filter, the ^{18}F -TFB was collected in a product vial preloaded with an additional 5 mL of saline.

Quality Control

The product ^{18}F -TFB was analyzed for radiochemical purity by both radio-TLC (MeOH, $R_f = 0.8$ – 0.85) and anion chromatography HPLC with a radioactivity detector (retention times, 3.7 min for ^{18}F -fluoride, 7.8 min for ^{18}F -TFB). Chemical purity, radiochemical identity, and specific activity were analyzed by anion chromatography HPLC (retention times, 3.5 min for fluoride, 4.3 min for chloride, 7.6 min for ^{19}F -TFB [conductivity]). Residual organic solvents were analyzed by gas chromatography.

In Vivo Imaging

Studies with mice were performed under approval of the Mayo Clinic Institutional Animal Care and Use Committee. Dynamic PET was performed in hNIS-expressing C6-glioma xenografted athymic mice after retroorbital injection of approximately 1.1 MBq of Na ^{18}F -TFB at different specific activities (10–0.001 mg of TFB/kg

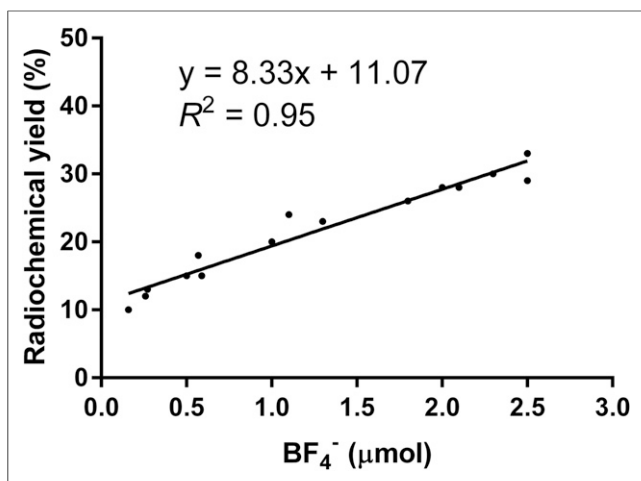


FIGURE 2. Relationship of radiochemical yields (uncorrected) to amount of unlabeled BF_4^- produced as found using different amounts of MP-64 resin to prefilter the BF_3 -tetrahydrofuran/petroleum ether reagent (data from Table 1).

mouse) to assess hNIS activity with ^{18}F -TFB. In this xenograft model, one flank had an hNIS-negative C6-glioma tumor xenograft, and the other flank had hNIS-expressing C6-glioma xenograft.

PET scans were acquired for 60 min followed by an x-ray scan using the GENISYS4 PET imaging system (Sofie Biosciences). The images from 40 hNIS-expressing C6-glioma xenografted mice were analyzed for SUV in the tumor, stomach, and thyroid using AMIDE image processing software (17). The SUV in the tumor was normalized with SUV in the stomach to account for difference in ^{18}F -TFB bioavailability in different animals due to competing uptake in normal organs such as thyroid, salivary glands, and stomach.

Immunohistochemistry

Tumors from 5 age-matched hNIS-expressing C6-glioma xenografted mice were harvested and formalin-fixed. The tumors were then equilibrated in 15% and 30% sucrose with phosphate buffer for 4 d, and frozen for cryosectioning. A series of adjacent sections were cut on a cryostat. Each section was 10- μm thick and mounted onto charged slides (Superfrost Plus slides; Fisherbrand). After being dried, the sections were blocked with 10% goat serum for 4 h at room temperature, followed by overnight incubation with 1:4,000 dilution of rabbit antihuman NIS antibody SJ1 (Imanis Life Sciences) in phosphate-buffered saline (PBS) with 10% goat serum at 4°C. The sections were rinsed 3 times in PBS-polysorbate 20 (0.05%) for 15 min each at room temperature. The sections were incubated with secondary antibody, Alexa Fluor 488 goat antirabbit IgG (H + L) antibody (Life Technologies), at a dilution of 1:4,000 in PBS for 45 min at room temperature. Following incubation with secondary antibody, the sections were rinsed 3 times in PBS-polysorbate 20 (0.05%) for 15 min each at room temperature. Subsequently, the sections were counterstained with nuclear stain, 4',6-diamidino-2-phenylindole (DAPI). The sections were then cover-slipped with mounting medium and imaged using a Nikon Eclipse Ti inverted microscope at 10 \times magnification.

Data Analysis and Statistics

Data are mean \pm SD. Microsoft Excel Solver was used to regress the tumor-to-stomach ratios of ^{18}F -TFB uptake using a nonlinear least-squares regression algorithm.

RESULTS

Radiosynthesis and Quality Control of ^{18}F -TFB

^{18}F -TFB was successfully produced by radiofluorination of BF_3 by passing a BF_3 -containing solution through a QMA cartridge preloaded with ^{18}F -fluoride and dried with acetone and nitrogen. The amount of

TABLE 1

Dependence of Overall Radiochemical Yield and Specific Activity ($n = 3$) of ^{18}F -TFB Product on Amount of Lewatit MP-64 Resin

Lewatit MP-64 resin (mg)	Unlabeled BF_4^- (μmol)	Uncorrected radiochemical yield (%)
0	8.33 ± 0.65	35.0 ± 3.6
200	2.43 ± 0.12	30.7 ± 2.1
250	1.97 ± 0.15	27.3 ± 1.2
300	1.13 ± 0.15	22.3 ± 2.1
350	0.55 ± 0.05	16.0 ± 1.7
400	0.23 ± 0.06	11.7 ± 1.5

Reactions were performed with starting ^{18}F -fluoride radioactivities of 15–37 MBq.

starting BF_3 for the reaction was found to be critical to determine both the radiochemical yields and the specific activities. First, 5 mL of BF_3 -tetrahydrofuran/petroleum ether solution ($\sim 45 \mu\text{mol}$) were used in the reaction, and $8.33 \pm 0.65 \mu\text{mol}$ unlabeled TFB with $35.0\% \pm 3.6\%$ yields were obtained. To decrease the amount of BF_3 for the reaction, the BF_3 -tetrahydrofuran/petroleum ether solution was passed through Lewatit MP-64 resin immediately before passage through the QMA cartridge. Lewatit MP-64 is an anion exchange resin, which contains cross-linked polystyrene matrix with tertiary amine and quaternary ammonium functional groups. Separate analysis of the post-Lewatit MP-64 filtrate showed that 70%, 80%, and 90% of the BF_3 in the original 5 mL of BF_3 -tetrahydrofuran/petroleum ether solution were retained on 200, 300, and 400 mg of Lewatit MP-64 resin, respectively. Thus, Lewatit MP-64 resin effectively reduced the amount of BF_3 reactant available for the reaction. Investigations with 200–400 mg of Lewatit MP-64 resin (Table 1) resulted in the production of unlabeled TFB and product ^{18}F -TFB in proportional amounts (Fig. 2). Thus, the specific activity of the ^{18}F -TFB product improved as the amount of Lewatit MP-64 resin was increased, however, at the cost of decreased radiochemical yield.

We chose to use 300 mg of Lewatit MP-64 resin for a high-radioactivity-level synthesis (40–44 GBq) as a compromise between radiochemical yield and specific activity. The radiochemical yield of ^{18}F -TFB was $20.0\% \pm 0.7\%$ ($n = 3$) uncorrected in a synthesis time of 10 min. Radiochemical purity was greater than 98% as shown on silica gel radio-TLC (supplemental data; Fig. 3) and anion chromatography HPLC (Fig. 3). Specific activities of $8.84 \pm 0.56 \text{ GBq}/\mu\text{mol}$ ($n = 3$) were achieved from starting ^{18}F -fluoride activities of 40–44 GBq.

Residual acetone and tetrahydrofuran were obtained in concentrations of 63–135 and 24–27 ppm (supplemental data; Fig. 4), respectively, which were well under the allowed solvent concentration limits (acetone, 5,000 ppm; tetrahydrofuran, 720 ppm) set by the International Conference on Harmonization for technical requirements for registration of pharmaceuticals for human use.

Stability of ^{18}F -TFB

Production samples stored for longer than 20 h at room temperature showed radiochemical purities greater than 96% on radio-TLC and HPLC. A slow release of ^{18}F -fluoride was observed, presumably

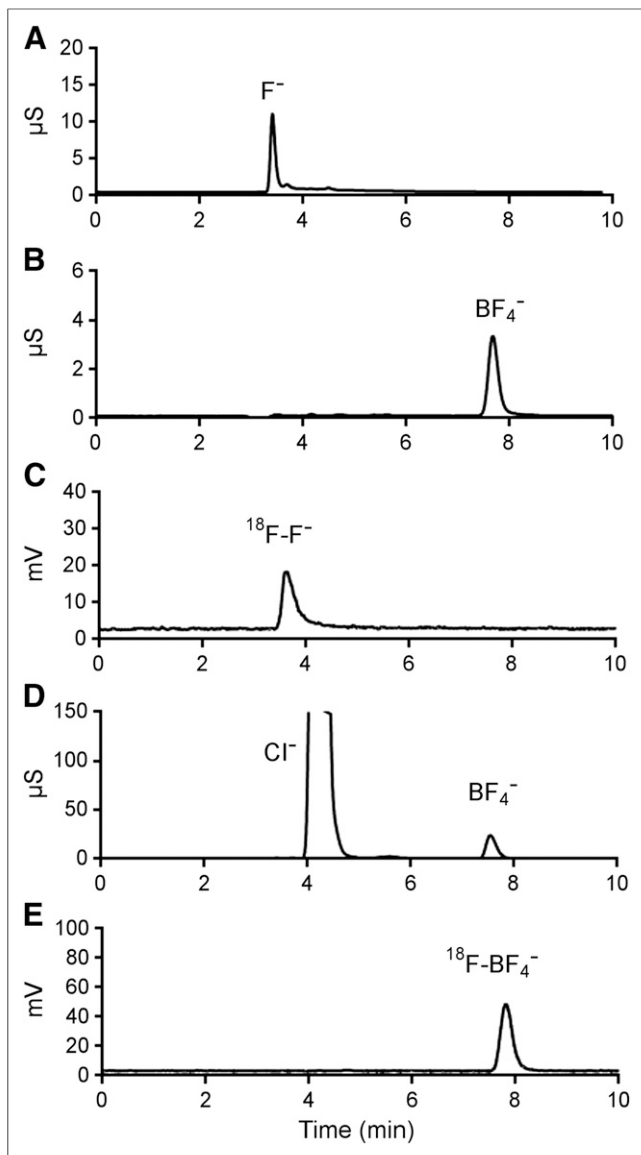


FIGURE 3. HPLC analysis of ^{18}F -TFB product in saline. (A) Conductivity data for 10 $\mu\text{g}/\text{mL}$ NaF standard. (B) Conductivity data for 10 $\mu\text{g}/\text{mL}$ NaBF_4 standard. (C) Radioactivity data for 1.1 MBq of ^{18}F -fluoride standard. (D) Conductivity data for purified ^{18}F -TFB in saline. (E) Radioactivity data for purified ^{18}F -TFB in saline.

reflecting a slow hydration of ^{18}F -TFB. HPLC analysis of a NaBF_4 stock solution stored for 7 mo at room temperature showed 50% of TFB had converted to fluoride.

In Vivo Imaging Studies

Robust uptake of ^{18}F -TFB was observed in the thyroid, stomach, bladder, and hNIS-expressing tumors of the C6-glioma xenograft mouse model (Figs. 4 and 5). No uptake of ^{18}F -TFB was observed in hNIS-negative tumors, confirming specificity of uptake of ^{18}F -TFB to hNIS-expressing tumors. ^{18}F -TFB uptake in the thyroid and hNIS-expressing tumor showed a biphasic kinetic: rapid uptake over the first 10 min was followed by slower uptake until 30 min with little subsequent change. The stomach showed linear increase in ^{18}F -TFB uptake over 60 min. Stomach uptake was independent of specific activity of ^{18}F -TFB whereas uptake in hNIS-expressing tumor and

thyroid was dependent on specific activity of ^{18}F -TFB. The uptake of ^{18}F -TFB by hNIS-expressing tumor was higher at high specific activity ($>13 \text{ MBq}/\mu\text{mol}$) than lower specific activity ($3 \text{ MBq}/\mu\text{mol}$). This trend was also seen for the thyroid. No evidence of bone uptake of ^{18}F radioactivity was seen, corroborating previous findings of negligible *in vivo* defluorination of ^{18}F -TFB in mice (14).

For a more detailed analysis of the effect of specific activity of ^{18}F -TFB on uptake in hNIS-expressing tumors, a 60-min time point was chosen, and a range of specific activities (10–0.001 mg of TFB injected/kg mouse weight) was tested. The uptake in tumor was normalized to stomach uptake to account for differences in bioavailability of ^{18}F -TFB across animals. The uptake of ^{18}F -TFB in hNIS-expressing C6 tumor showed dependence on specific activity at 10–0.5 mg of TFB/kg of mouse weight or 0–10 $\text{MBq}/\mu\text{mol}$ considering approximately 1.1-MBq radioactivity injected in approximately 25-g mice. But this trend was not observed for higher specific activities ($>10 \text{ MBq}/\mu\text{mol}$ TFB or $<0.5 \text{ mg TFB}/\text{kg}$ mouse weight) (Fig. 6). At these higher specific activities, the uptake of ^{18}F -TFB was no longer dependent on specific activity but exhibited high variability. Immunohistochemistry analysis for hNIS in tumor sections from 5 mice showed significant intratumoral and intertumoral variability of expression of hNIS (Fig. 7) that may play a role in the variability of ^{18}F -TFB uptake observed in tumors.

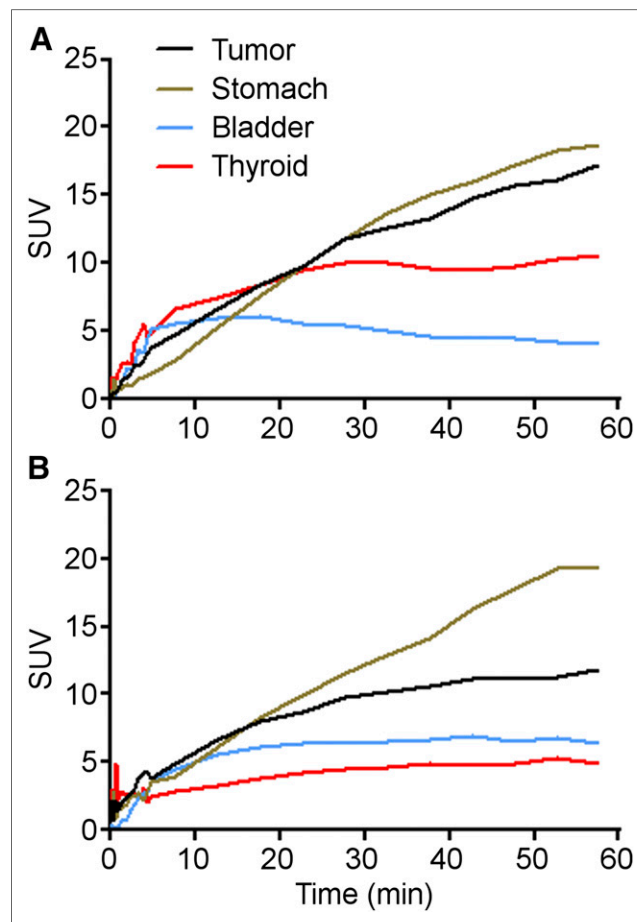


FIGURE 4. Time dependence of ^{18}F -TFB uptake (SUV) in different organs in representative hNIS-expressing C6-glioma xenografted mice at high specific activity of ^{18}F -TFB (13 $\text{MBq}/\mu\text{mol}$ or 0.37 mg/kg mouse weight) (A) and low specific activity of ^{18}F -TFB (3 $\text{MBq}/\mu\text{mol}$ or 1.6 mg/kg mouse weight) (B).

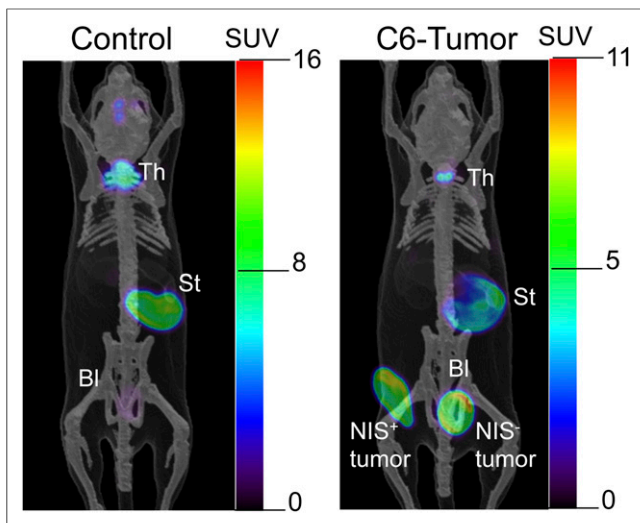


FIGURE 5. PET images of ^{18}F -TFB distribution at 60–70 min in control mouse (left) and mouse bearing hNIS-positive and hNIS-negative C6-glioma xenografts. Overlaid reference bone atlas is computer generated. Bl = bladder; St = stomach; Th = thyroid.

DISCUSSION

It has been proposed that the ^{18}F -labeled iodide analog ^{18}F -TFB may have high utility as an hNIS gene reporter probe for PET studies (14); however, the existing isotope exchange labeling method rendered the product with moderate specific activity. Because BF_3 is known to form TFB in the presence of water via a fluoride exchange reaction (18,19), we aimed to use this reaction to prepare high-specific-activity ^{18}F -TFB. By the new methodology, specific activities of $8.84 \pm 0.56 \text{ GBq}/\mu\text{mol}$ and uncorrected radiochemical yields of $20.0\% \pm 0.7\%$ were obtained with a starting activity of 40–44 GBq. Further modifications of the method can produce even higher-specific-activity ^{18}F -TFB at the sacrifice of radiochemical yield, or higher radiochemical yield at the sacrifice of lower specific activity (Table 1). The highest specific activity obtained by acid-catalyzed ^{18}F -fluoride exchange on TFB was approximately $1 \text{ GBq}/\mu\text{mol}$, with starting activities of 12–18 GBq of ^{18}F -fluoride, and the radiochemical yield was approximately 10% (14).

Jauregui-Osoro et al. (14) estimated that the administration of approximately 400 MBq of ^{18}F -TFB synthesized by the conventional method to a human subject would result in a plasma concentration of approximately $0.1 \mu\text{M}$ TFB. Considering the half maximal inhibitory concentration (IC_{50}) of TFB to be $0.1\text{--}1 \mu\text{M}$ for inhibition of iodine uptake by NIS in the thyroid (20), it is desirable to increase ^{18}F -TFB specific activity above approximately $5 \text{ GBq}/\mu\text{mol}$ to avoid a pharmacologic effect (14). The presently reported synthesis method for ^{18}F -TFB achieves this goal. At a specific activity of $8 \text{ GBq}/\mu\text{mol}$, an approximately 400-MBq administered dose of ^{18}F -TFB would give an estimated in vivo concentration of approximately $0.02 \mu\text{M}$ TFB, which should not exhibit a pharmacologic effect.

To evaluate the influence of ^{18}F -TFB specific activity on in vivo uptake by NIS-expressing tissues, we used an hNIS-expressing C6 tumor xenograft mouse model. As expected, ^{18}F -TFB was taken up by selected organs expressing NIS in the xenograft mouse model. Among the select organs, thyroid and hNIS-expressing tumor were sensitive to a specific activity of ^{18}F -TFB as ^{18}F -TFB was being transported using NIS in these organs. On the

other hand, in the stomach, which also possesses NIS (21–23), the uptake of ^{18}F -TFB was found to be independent of its specific activity. The insensitivity of ^{18}F -TFB uptake to specific activity in the stomach was not clarified but may point to different kinetic properties of the NIS protein in gastric mucosal cells as compared with thyroid and hNIS-expressing tumor (22,23). Another possible explanation is that ^{18}F -TFB entering the gastric epithelial cells is immediately effluxed into the stomach lumen such that the intracellular concentration (e.g., in gastric parietal cells) is never in equilibrium with the interstitial fluid so unidirectional transport continues unabated. A biphasic response was observed in hNIS-expressing tumor uptake of ^{18}F -TFB versus administered dose of unlabeled TFB. The ^{18}F -TFB uptake in tumor decreased with increasing amount of administered TFB over the range of 0.5–10 mg TFB/kg of mouse weight, but this trend was not observed for higher specific activities ($<0.5 \text{ mg TFB/kg}$ of mouse weight).

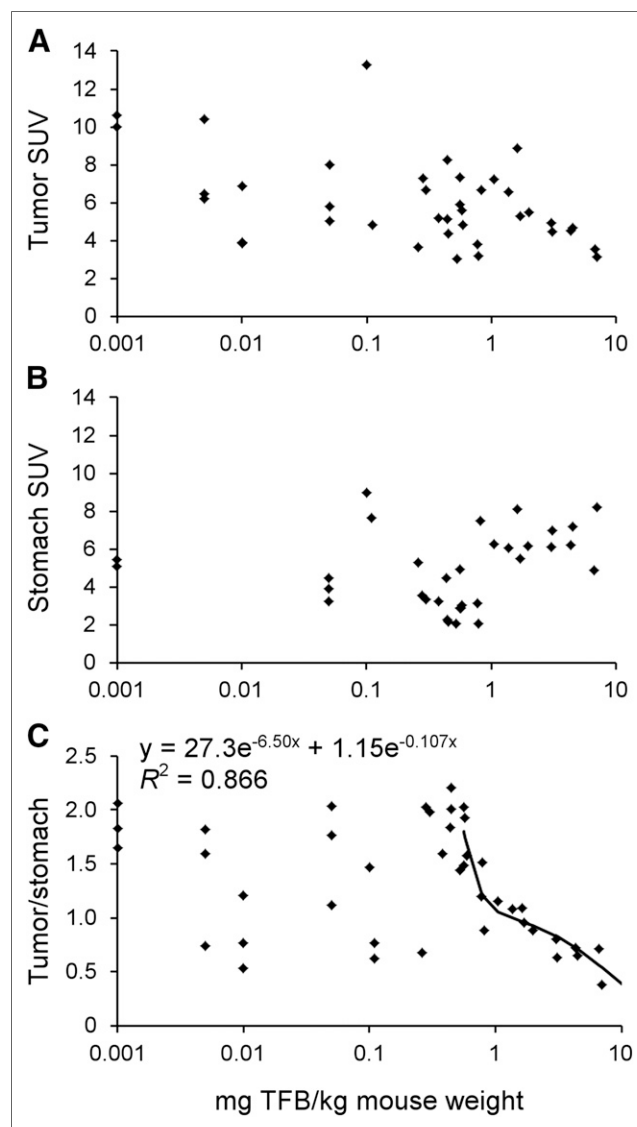


FIGURE 6. Dependence of tumor (A), stomach (B), and tumor-to-stomach ratio (C) of ^{18}F -TFB uptake at 60–70 min on administered mass of TFB to hNIS-expressing C6-glioma xenografted mice. Tumor-to-stomach ratio data for administered mass greater than 0.5 mg/kg was fit to biexponential clearance model using nonlinear least-squares regression.

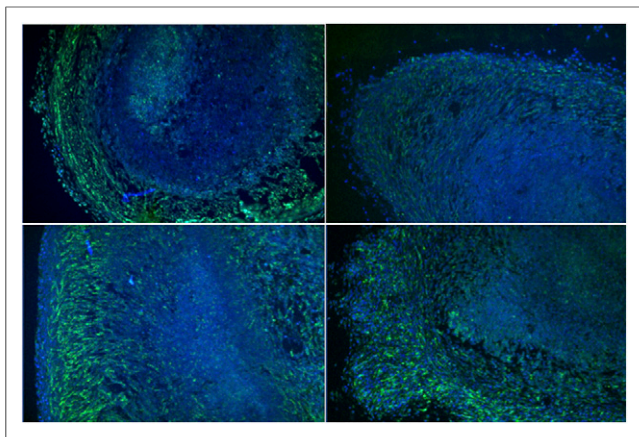


FIGURE 7. Immunostaining of hNIS-expressing C6-glioma xenografts (10× magnification) showing intratumoral and intertumoral variability of expression of hNIS. Blue = DAPI-stained nucleus; green = Alexa Fluor 488 antibody-bound hNIS.

Rather, the tumor uptake was constant but highly variable for administered TFB doses of less than 0.5 mg/kg. The reason for this trend is not clear, but it is possible that at high specific activity, factors other than specific activity contribute to the variability, such as variability in the inter- and intratumoral expression or activity of hNIS, number of tumor cells expressing hNIS, heterogeneity of tumor perfusion or oxygenation, variability of tumor size, or the indirect influence of differences in the physiologic distribution of radiotracer to other areas of the body. The large variation seen in hNIS expression levels in the C6-glioma xenografts may reflect the fact that the C6-hNIS-transduced cell line was not a clonal population but included high-, low-, and negative-expressing cells. The ability of the ^{18}F -TFB PET method to reliably report on viral infection depends on hNIS expression within infected cells and possibly posttranslational events that influence hNIS transporter activity (24). These considerations must also be kept in mind for future studies in monitoring hNIS transduction in human studies that may also entail significant heterogeneity of hNIS expression after viral therapies. Nonetheless, it was encouraging to observe a broad range of specific activities of ^{18}F -TFB over which tumor uptake was robust.

CONCLUSION

A solid-phase supported synthesis of ^{18}F -TFB was developed via radiofluorination of BF_3 . With the optimized condition, the radiochemical yield of ^{18}F -TFB was $20.0\% \pm 0.7\%$ ($n = 3$) uncorrected in a synthesis time of 10 min. Specific activities of $8.84 \pm 0.56 \text{ GBq}/\mu\text{mol}$ ($n = 3$) were achieved with starting ^{18}F -fluoride radioactivities of 40–44 GBq. A positive correlation was observed between specific activity of ^{18}F -TFB and hNIS-expressing C6-glioma xenografts for lower specific activities resulting in administration of TFB exceeding 0.5 mg/kg in mice. The increased specific activity of ^{18}F -TFB may allow for enhanced PET imaging of hNIS reporter in future human studies.

DISCLOSURE

The costs of publication of this article were defrayed in part by the payment of page charges. Therefore, and solely to indicate this fact, this article is hereby marked “advertisement” in accordance

with 18 USC section 1734. The work was supported by the Department of Radiology, Mayo Clinic. No other potential conflict of interest relevant to this article was reported.

ACKNOWLEDGMENTS

We thank Benjamin C. Jager for the analysis of PET images and Ping Fang for the support of ^{18}F -fluoride production and gas chromatography analyses.

REFERENCES

1. Chung JK. Sodium iodide symporter: its role in nuclear medicine. *J Nucl Med.* 2002;43:1188–1200.
2. Penheiter AR, Russell SJ, Carlson SK. The sodium iodide symporter (NIS) as an imaging reporter for gene, viral, and cell-based therapies. *Curr Gene Ther.* 2012;12:33–47.
3. Ahn BC. Sodium iodide symporter for nuclear molecular imaging and gene therapy: from bedside to bench and back. *Theranostics.* 2012;2:392–402.
4. Daniels GH, Haber DA. Will radioiodine be useful in treatment of breast cancer? *Nat Med.* 2000;6:859–860.
5. Dai G, Levy O, Carrasco N. Cloning and characterization of the thyroid iodide transporter. *Nature.* 1996;379:458–460.
6. Eskandari S, Loo DD, Dai G, Levy O, Wright EM, Carrasco N. Thyroid Na^+/I^- symporter: mechanism, stoichiometry, and specificity. *J Biol Chem.* 1997;272:27230–27238.
7. Sparagana M, Little A, Kaplan E. Rapid evaluation of thyroid nodules using $^{99\text{m}}\text{Tc}$ -pertechnetate scanning. *J Nucl Med.* 1970;11:224–225.
8. Ryo UY, Vaidya PV, Schneider AB, Bekerman C, Pinsky SM. Thyroid imaging agents: a comparison of I-123 and Tc-99m pertechnetate. *Radiology.* 1983;148:819–822.
9. Groot-Wassink T, Aboagye EO, Wang Y, Lemoine NR, Reader AJ, Vassaux G. Quantitative imaging of Na/I symporter transgene expression using positron emission tomography in the living animal. *Mol Ther.* 2004;9:436–442.
10. Schmitz J. The production of ^{124}I -iodine and ^{86}Y -yttrium. *Eur J Nucl Med Mol Imaging.* 2011;38:S4–S9.
11. Anbar M, Guttman S, Lewitus Z. The accumulation of fluoroborate ions in thyroid glands of rats. *Endocrinology.* 1960;66:888–890.
12. Anbar M, Guttman S, Lewitus Z. Effect of monofluorosulphonate, difluorophosphate and fluoroborate ions on the iodine uptake of the thyroid gland. *Nature.* 1959;183:1517–1518.
13. Anbar M, Guttman S. The isotopic exchange of fluoroboric acid with hydrofluoric acid. *J Phys Chem.* 1960;64:1896–1899.
14. Jauregui-Osoro M, Sunassee K, Weeks AJ, et al. Synthesis and biological evaluation of F-18 tetrafluoroborate: a PET imaging agent for thyroid disease and reporter gene imaging of the sodium/iodide symporter. *Eur J Nucl Med Mol Imaging.* 2010;37:2108–2116.
15. Weeks AJ, Jauregui-Osoro M, Cleij M, Blower JE, Ballinger JR, Blower PJ. Evaluation of F-18 tetrafluoroborate as a potential PET imaging agent for the human sodium/iodide symporter in a new colon carcinoma cell line, HCT116, expressing hNIS. *Nucl Med Commun.* 2011;32:98–105.
16. Youn H, Jeong JM, Chung JK. A new PET probe, F-18-tetrafluoroborate, for the sodium/iodide symporter: possible impacts on nuclear medicine. *Eur J Nucl Med Mol Imaging.* 2010;37:2105–2107.
17. Loening AM, Gambhir SS. AMIDE: a free software tool for multimodality medical image analysis. *Mol Imaging.* 2003;2:131–137.
18. Wamser CA. Equilibria in the system boron trifluoride-water at 25 °C. *J Am Chem Soc.* 1951;73:409–416.
19. Wamser CA. Hydrolysis of fluoboric acid in aqueous solution. *J Am Chem Soc.* 1948;70:1209–1215.
20. Lecat-Guillet N, Ambroise Y. Discovery of aryltrifluoroborates as potent sodium/iodide symporter (NIS) inhibitors. *ChemMedChem.* 2008;3:1207–1209.
21. Portulano C, Paroder-Belenitsky M, Carrasco N. The Na^+/I^- symporter (NIS): mechanism and medical impact. *Endocr Rev.* 2014;35:106–149.
22. Wolosin JM. Ion transport studies with H^+/K^+ -ATPase-rich vesicles: implications for HCl secretion and parietal cell physiology. *Am J Physiol.* 1985;248:G595–G607.
23. Harden RM, Alexander WD, Shimmins J, Chisholm D. A comparison between the gastric and salivary concentration of iodide, pertechnetate, and bromide in man. *Gut.* 1969;10:928–930.
24. Kogai T, Brent GA. The sodium iodide symporter (NIS): regulation and approaches to targeting for cancer therapeutics. *Pharmacol Ther.* 2012;135:355–370.